FULL LENGTH PAPER

METHODOLOGY FOR SIMULTANEOUS SIMULATION OF CONVECTIVE AND RADIATIVE HEATING

B. Chiranjeevi Phanindra; S. Jeyarajan; R. Manoj; K. Vanitha; John G. Geo; B. Deependran and M.J. Chacko
Vikram Sarabhai Space Centre
Indian Space Organisation, ISRO Post
Thiruvananthapuram-695 022, India
Email :

Abstract

During the ascent flight of a Launch Vehicle (LV), certain regions are exposed to radiative and convective heating simultaneously. A typical example is the flexible multilayer thermal barrier for launch vehicle base region which experiences both radiative heating from the plume and hot nozzle divergent as well as convective heating due to reverse flow. To design and evaluate the effectiveness of the thermal barrier, simultaneous simulation of both radiative and convective heating is essential. This was made possible by the utilization of controlled radiant heaters and a Convective Heating System (CHS), both acting simultaneously in a pre-designated sequence. Such a simulation is very challenging since, the simultaneous simulation of radiative heating and convective heating mutually interferes with their respective independent control systems. Besides, the influence of the boundary conditions in the heat transfer process is different for radiative and convective heating. Hence, a novel technique was adopted to isolate the respective control systems. Detailed tests were undertaken to map the flow field at various distances from the exit to determine the position of the test article. After extensive mapping, the facility was utilized for simulations of both radiative and convective heating simultaneously on a thermal protection element in the launch vehicle base region, which experiences simultaneous simulation of convective and radiative heating. The studies were able to bring out the effect of hot gas permeability and thermal response and ascertain that the back wall temperatures are within allowable temperature constraint. This mode of simulation is a new technique where both simultaneous simulation of convection and radiation was undertaken to simulate the actual environments of flight on a specific system

Nomenclature

CHS = Convective heating system
h = Heat transfer coefficient
Q = Heat flux
Q_m = Measured heat flux
T_g = Plume temperature
T_w = Wall temperature
T_{w1} = Wall temperature of Gardon gauge

Introduction

During flight, Launch Vehicles (LV) experience heating from various modes. Certain regions are subjected to convective heating as in the case of aerodynamic heating on external surfaces while certain regions are subjected to radiation heating as in the case of nozzle radiation on plumb lines, inter stage structure etc. There are also instances where both radiative and convective heating are simultaneously acting on LV structures such as base heating, where both radiation from nozzle divergent and plume together with convective heating from reverse flow are acting.

In the base region of a launch vehicle, the strap-on thermal shroud protects the structure and the inside elements from base heating. This flexible member is called thermal boot which facilitates free gimballing of the nozzle situated at the base of launch vehicle. Base heating is in the form of radiative heating from solid motor exhaust plumes and from liquid engine nozzle divergent, and convective heating due to reverse flow or direct plume

Paper Code : V66 N4/822-2014. Manuscript received on 19 Jun 2013. Reviewed, revised and accepted as a Full Length Contributed Paper on 09 Sep 2014

impingement from adjacent nozzle. So the flexible multi-layer insulation must be provided with hot gas impermeability to protect the interior components from both types of heating. To evaluate its effectiveness, simulation of both radiative and convective heating is necessary to be carried out simultaneously as it occurs in flight.

Radiative heating was simulated using the Infrared heater module. To simulate the convective heating over a specimen the Convective Heating System (CHS) was realized.

Different experimental setups are built for simulation of convective heating. One such set up is the hypersonic wind tunnel at the Langley Aerothermodynamic Laboratory. The test gas in these tunnels is heated, dried and filtered air [1].

Arc jet heating is another method for convective heating. But there are instances, where both simultaneously convection and radiation have to be simulated. Normally it is not possible to simulate radiative heating conditions in the arc-jet. Hence, generally testing is done in a convective environment, at heating rates representative of the total (convective plus radiative) heating rates and heat loads [2].

LeBel et al. [3] reported the usage of oxy-acetylene torch as a heat source for laboratory tests. Heating conditions were varied by adjusting nozzle size, distance from nozzle to sample, and gas composition. They have achieved heating rates from 100 to 300 W/cm^2 with run times up to 80s.

Koo et al. [4] developed a supersonic torch facility for ablative material testing and it was later renamed as the Simulated Solid Rocket Motor (SSRM). The SSRM is a small-scale, liquid-fueled rocket motor burning kerosene oxygen. Aluminum oxide particles are injected into the plume to simulate the particle-laden flow of solid rocket exhaust. The SSRM is a controlled laboratory device capable of producing a particle-laden exhaust environment with measured heat fluxes from 284 to 1,370 W/cm^2. The flame temperature is approximately 2,200°C and the velocity of the particle-laden exhaust is approximately 2,000 m/s.

Ames Entry Heating Simulator houses the facility to simultaneously simulate convective and radiative heating [5]. The convective heating is simulated by a wind tunnel with an arc-heated supersonic stream, while the radiative heating is applied by a carbon-arc radiation source and two ellipsoidal mirrors. The drawback in this kind of setup is that the back wall of the test article will be heated, which might not be of concern for thin long cylindrical test articles. But the heating from the back is not acceptable while studying the thermal response of test articles like silica tile testing exposed to external heating. Also, in case of rectangular test articles the shadow of the test article will be projected on to the ellipsoidal mirror, which will reduce the heating or produce uneven heating.

Taking into account the difficulties encountered for the simultaneous simulation of radiative and convective heating, a facility was established with LPG burner for convective heating and a controlled high intensity infrared heater module for radiative heating.

The paper presents the details of the LPG fired CHS, aspects of detailed mapping of flow field, its integration to the radiative heating control, simultaneous simulation of the transient radiative heat flux and convective heat flux for evaluating the base thermal protection system. Mapping of heat flux was carried out using a Gardon type heat flux sensor which was calibrated in radiative environment. The error in measurement of convective heat flux with a gauge calibrated in radiative environment is about 10% according to Reference [6]. Study also evaluates the plume impingement effects on the thermal boot and study whether any surface layer gets damaged under the combined effect of radiative and convective heating. In the process, a methodology for simultaneous controlled simulation of both radiation and convection heating was brought out. The unique advantage of such simulation is that it has made possible the study of thermal response of multi-layer insulation systems with imperfect thermal contact and partial plume penetration, which otherwise would have been extremely cumbersome for numerical modeling.

Facility Description

Convective Heating System

Simulation of convective heating was carried out using Convective Heating System (CHS). CHS is a LPG (Liquefied Petroleum Gas) fired burner. The maximum power output of the burner is 100,000 kCal/h, while the motor capacity is 0.15 kW. The diameter of outlet is 88 mm. The CHS consists of LPG cylinders, pressure manifold, gate valve, solenoid valve, burner, blower and damper as shown in the block diagram given as Fig.1. The view of

the convective heating system during operation is shown in Fig.2.

Totally three LPG (19.4 kg) cylinders were used for firing. There is a provision on pressure manifold to connect 5 LPG cylinders in series. A gate valve at the exit of the manifold gives the provision to control the gas supply to the burner. Next to the gate valve is a pressure regulator to regulate the LPG pressure within the maximum input pressure of the burner. Fuel is supplied to burner through solenoid valve. A damper is provided over the air blower, which gives a provision to cut down the air supply to any ratio of its full opening, through which the air-fuel ratio of the combustion process can be varied. The electrical power to the burner goes through the control panel.

For using the LPG burner system for the simulation of controlled convective heating, a detailed characterizing of CHS was carried out. For this purpose, detailed measurements of different parameters like heat flux, velocity and plume temperature were carried out as described below.

Heat Flux Measurements

Heat Flux measurements were carried out with a calibrated Gardon type heat flux sensor.

Figure 3 gives the heat flux measurement at an axial location of 200 mm from CHS outlet for a period of 120s. The mean heat flux was observed to be increasing at all axial locations with respect to time. To qualify this measurement, temperature measurement was carried out at an axial location of 200 mm, which is given in the later section.

Convective Heat transfer is given by,

$$Q = h\,(T_g - T_w) \qquad (1)$$

For a fixed location and plume configuration, 'h' can be taken as constant. Since, the heat flux measurements were carried out with water cooled Gardon gauge, the wall temperature (T_w) can be taken as a constant value throughout the measurement. Hence, as the temperature of the plume (T_g) increases, which can be seen from Fig.4, the heat flux measurements also have the increasing trend.

Velocity Measurements

Velocity measurements were carried out with a pitot static probe which was connected to a differential pressure transducer. The probe was exposed to the jet after 60s of its operation, after the plume was stabilized. The velocity observed in the flow is 20 m/s at a distance of 250 mm with an error of ±2 m/s.

Temperature Measurements

Temperature measurements were carried out with stagnation temperature probe placed at different axial distances from the exit. The plume temperature (Fig.4) was observed to be increasing and stabilized at about 40s. Hence, the stable test conditions would be considered only after 40 - 60s of the burner operation. The flame temperature at an axial distance of 200 mm is about 1250°C.

Fluctuations in temperature measurements at an axial location of 200 mm can be observed from Fig.4. The reasons for the oscillating behavior of the temperature are explained as follows: The required axial pressure to the flame is being supplied from a rotary fan. The air supplied by a rotating fan is having an inherent unsteadiness in the flow field. From a Fast Fourier Transformation (FFT) of the pressure data, it was found that the single dominant frequency is closely corroborating with the fan speed. Besides, an intrusive flow field measurement technique will induce disturbance in the flow being measured.

Radiative Heating System

Simulation of radiative heat flux was achieved by exposing the test article to thermal radiation from an array of quartz enveloped tungsten filament infrared lamps. Transient variation of heat flux simulation was achieved by using Programmable Logic Control (PLC) based power controllers working in feedback mode. The heater modules have the capability of simulating 200 W/cm^2 incident heat flux. Fig.5 gives the block diagram of radiative heating system. The required heat flux profile will be fed to the PLC controller through a PC. A Gardon type heat flux sensor, which is placed at the same distance from the IR lamps as the test specimen is used to sense the radiation and is used for feedback control. After comparing the signals from feedback control and data input from PC, PLC controller gives the required signal to the thyristor, which provides the specified electric input to the IR lamps. The radiation emitted by the IR lamps is proportional to the electric input fed to the lamps. Thermocouples will be bonded on the back surface of the test specimen to study the thermal response of the test specimen. The thermal data from the heat flux sensor and the thermocouples will

be logged using a PC based Data Acquisition system. Fig.6 gives the view of radiative heater module.

Methodology for Simultaneous Simulation of Radiative and Convective Heating

Basic Difference in the Simulation of Radiative and Convective Heating

Black body absorbs the entire radiative energy incident on its body, all other materials absorb a fraction of energy incident on them which depend on their surface absorptivity. So, when the IR radiation is incident on a test article, it will absorb only an amount of radiation which is its absorptivity times the incident radiation. Thus, for simulating the convective heat flux using IR radiation it should be suitably augmented into radiative heat flux by a factor which is the reciprocal of the absorptivity of the material on which the convective heat flux is incident.

Similarly, for convective heating, the energy absorbed by the surface depends on the temperature difference between the hot gas and wall temperature. Hence, the increased wall temperature decreases the convective heat absorbed by the surface. These aspects are to be carefully considered for simulations.

Influence of Convective Heating on Radiative Heating Control

For simulating the transient radiative heat flux, a heat flux sensor was used during the test in feedback mode to the controller. The difficulty in using the feedback heat flux sensor in the present configuration is that the heat flux sensor will measure in addition the heat flux from the convective plume also. Because of which, the feedback gauge measures different heat flux than that from radiation alone, and hence the sensor feedback to controller and firing to the IR lamps in closed loop connection will be erroneous.

Strategy and Approach

The radiative heating was simulated using radiative heaters following the real time heat flux history for the entire test duration. The convective heat flux was simulated with plume impinging velocity of 20 m/s, density of 0.2402 kg/m^3 and total gage pressure of 35 N/m^2. The equivalent convective heating was simulated with a heating profile, such that the convective heat load is same as that of the required.

Initially, trial tests were undertaken to map the heat flux history and evaluate the feasibility of undertaking the above test. A trial test was carried out on a true test sample by radiative heating method, in which both radiative and convective heating was applied. Thermocouple was bonded on surface, to measure the surface temperature variation with time. The gas temperature variation with time was measured with a stagnation temperature probe. To fix the inclination angle and axial location of specimen with respect to CHS, a Gardon type heat flux sensor, mounted flush on a silica tile as shown in Fig.6 was used. The required convective heat flux to be simulated on the specimen was calculated as below.

Absorbed convective heat flux on the specimen is given by Eq.(1). However, the heat flux being measured with Gardon gauge is,

$$Q_m = h\,(T_g - T_{w1}) \tag{2}$$

Since, heat flux was measured with water cooled Gardon gauge, T_{w1} is taken as 303 K. From Eq.(2), the heat transfer coefficient was obtained.

The heat transfer coefficient 'h' is assumed to be the same for the same flow configuration and axial location even if the surface temperature of the test article changes. Hence, from the measured plume and surface temperatures and required convective heat flux, the heat flux required to be measured by the heat flux sensor was derived from eqs(1) and (2) as follows.

$$Q_m = Q\,\frac{(T_g - 303)}{(T_g - T_w)} \tag{3}$$

The measured gas temperature at the point of simulation of convective heating was 1373 K, whereas the surface temperature of specimen was 580 K at the corresponding time. From Eq.(3), in order to make the specimen absorb the desired convective heat flux, the distance of the heat flux sensor and the heat flux to be measured was estimated. The silica tile with the heat flux sensor as shown in Fig.7 was placed in different inclinations and axial locations and the heat flux was measured. Silica tile was selected to be the sensor holder since, it is a high temperature insulator as required for the heat flux sensor and also it would simulate the actual flow field over the flat test sample leading to correct measurement of heat flux during actual test. The position of the specimen was fixed, where the heat flux sensor measured the required

heat flux using the corresponding 'h' for that location. Also, to measure the variation of heat flux along the length of the specimen, total 3 nos. of heat flux sensors, one at the center of the silica tile and remaining 2 nos. on either edges of the silica tile were used. The difference between the sensor near to CHS system and the center sensor was about 2 W/cm^2, whereas the difference between the center sensor and the sensor farther to CHS was about 0.5 W/cm^2.

To avoid the interference of convective heating on radiative heating control, two identical heater modules were used, one for simulation of actual radiative heat flux on the test article and the other of same power rating in parallel in remote location away from the influence of the convective source. The two heater modules (one in the test setup and the other in the remote location) were connected to same power controller, such that the power drawn by the two heater modules were same. The required heat flux was simulated with in feedback mode and the heat fluxes were measured for both the heater modules. During the actual test with both convection and radiation simulation, the gauge at the remote heater was used in feedback mode for the control of heat flux history.

Experimental Setup and Preparation of Test Specimen

The specimen inclination of 41° with the direction of plume and at a distance of 250 mm from the exit of CHS as shown in the schematic given in Fig.8 was found to be simulating the required convective heat load. At this position the radiative heater module was assembled parallel to the specimen for applying the transient radiative heating uniformly over the specimen.

The complete test setup is shown in Figs.9 and 10. Trial tests were undertaken to fix the position and inclination of the specimen with respect to the CHS and radiative heater module.

Tests were undertaken on a 150 mm x 150 mm test specimen of the flexible thermal barrier in the base region of the launch vehicle that experiences both radiative and convective heating. A 9 layer configuration comprising of Glass cloth, Silica cloth, Aluminized Silica cloth and Rubber layer was used as the test sample. Fig.11 shows the configuration of the test sample.

K-type thermocouples were bonded at the back wall of layers 3 (Silica cloth), 4 (Silica cloth), 5 (Heatlab) and 8 (Rubber). Also, three K-type thermocouples were bonded at the back wall of test specimen as shown in Fig.12.

Test Procedure and Results

Two different tests were carried out on similar specimens. Test 1 was carried out by simultaneous simulation of an equivalent convective heat load and transient radiative heat flux on the test specimen. Fig.13 gives the pictorial view during test, showing specimen being heated by IR heater module and plume impingement heating from CHS. A similar test was carried out to measure the total heat flux with a sensor flushed in a silica tile. The convective heat flux measured with the Gardon gauge (Q_m) was corrected to the heat flux (Q) applied on specimen from Eq.(3). Though, the source temperature in flight (1600 to 1856 K) and source temperature in lab (1418 K) are different, it is not substantial as to cause physical differences in flow phenomenon. Hence, the thermal response of the material will not be different from the actual flight scenario. The simulation of convective heat load was carried out to match the estimated cold wall heat load. But, the hot wall heat load in flight is less than that simulated in the lab. Thus, the lab simulation is conservative and hence to that extent the thermal response of the material generated in lab will be higher than that of flight. Fig.14 gives the comparison of required and simulated convective and radiative heating in terms of non-dimensional numbers.

Test 2 was carried out applying the radiative heating over the specimen using the high intensity infrared heater module, which is a combination of direct radiative heating and radiative heating augmented by absorptivity to simulate the convective heat load.

Figure 15 gives the thermal response of various in depth locations and back wall of flexible thermal barrier specimen in test 1. The maximum back wall temperature measured was 106°C. The maximum interface temperature on rubber was 108°C.

Backwall of 3rd layer (silica cloth) was the most exterior temperature measurement from the tests. The transient variation of the temperature can be related with the heat flux profile simulated over the specimen. The temperature profile has a constant slope till 45s, where only constant radiative heat flux was simulated. At 80s, the convective heating was started and simultaneous convective and radiative heating were acting on the specimen. Thus, the slope of the temperature curve showed an increase trend.

The immediate rise in temperature is due to partial plume penetration into the inner layers, as the glass cloth and silica fabric are permeable. The applied convective and radiative heating have less impact on the temperatures on interior layers such as rubber. The same is observed on specimen backwall also as rubber provides an impermeable barrier for hot gas penetration. Rather the rise in temperature was through conduction and inter layer radiative exchange.

Test 2 results show that the back wall temperature of rubber had reached 103°C, while the specimen back wall reached 97°C at the end of the test. Table-1 gives the comparison of thermal response of the specimen in test 1 and 2. The backwall temperature with full radiation test is lower because emission loss is more, whereas in the combined convection-radiation mode, the radiative loss is less showing a higher temperature of 106°C. Also, the hot plume can penetrate the inner layers and heat it differently from that of a pure radiation scenario. This brings out the effect of convective plume impingement in comparison to a purely radiative heating. Fig.16 gives the photographic views of the specimen before and after the test. The specimen was physically intact, while the top layer (glass cloth) was slightly discolored.

Thus, through the simultaneous simulation of both radiative and convective heating, it was made possible to study the thermal response of multilayered insulation system with imperfect thermal contact and partial plume penetration.

Conclusions

- A new methodology for simultaneous simulation of radiative and convective heating was evolved and demonstrated. For this a convective heating system was established for simulating the plume impingement effects on the test specimen. Radiation was simulated using a high intensity infrared heater module which was controlled through a PLC based power controller. Correction steps are designed for excluding the effect of convective heating on temperature sensors.
- Extensive mapping of the flow field and incident radiation were undertaken to establish the heating levels. Typical thermal response studies were undertaken on a test sample of base thermal barrier system.
- The maximum back wall temperature measured in the present test was 106C. After the test, the specimen was found physically intact.
- The results were compared with the thermal response for that of a purely equivalent radiative heating and the effect of plume penetration in to the inner layers were understood.
- This novel method of simulating both convective and radiative heating simultaneously has enabled the study of thermal response of MLI with imperfect thermal contact and plume penetration, which otherwise would have been extremely cumbersome for numerical modeling.

Table-1 : Comparison of Thermal Response During Different Tests

	Combined Convection and Radiation Test	Pure Radiation Test
Backwall of Rubber Temperature (°C)	108	103
Specimen Backwall Temperature (°C)	106	97

Acknowledgement

Authors would like to thank Mr. R. Sreekumar, Mr. K. Prajoob and Mr. P. Satheesh for their support during test specimen preparation, assembly and testing.

References

1. Thomas J. Horvath., "Experimental Aerothermodynamics in Support of the Columbia Accident Investigation", AIAA, 2004-1387.

2. Kristina Skokova and Bernard Laub., "Experimental Evaluation of Thermal Protection Materials for Titan Aerocapture", AIAA, 2005-4108.

3. LeBel, P. J., Russell III, J. M., "Development of Ablation Sensors for Advanced Reentry Vehicles", 20th Annual ISA Conference and Exhibit, Los Angeles, CA, October, 4-7, 1965.

4. Chaboki, A., and Koo, J. H. et al., "Supersonic Torch Facility for Ablative Testing," AIAA-90-1761, June, 1990.

5. Lundell, J. H., Wakefield, R. M. and Jones, J. W., "Experimental Investigation of a Charring Ablative Material Exposed to Combined Convective and Radiative Heating in Oxidizing and Nonoxidizing Environments", NASA-TM-X-54797, 19640101, January, 1, 1964.

6. Borell, G.J. and Diller, T.E., "A Convective Calibration Method for Local Heat Flux Gages", ASME Journal of Heat Transfer, Vol.109, pp.83-89, February, 1987.

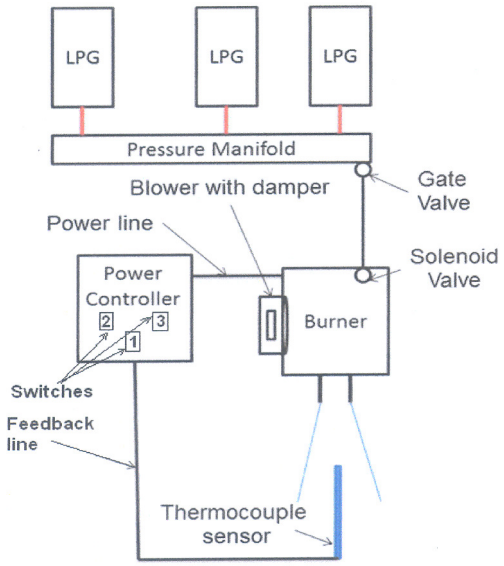

Fig.1 Block Diagram of Convective Heating Source System

Fig.2 Photographic Views of Gardon Gauge Heat Flux Sensor in Plume

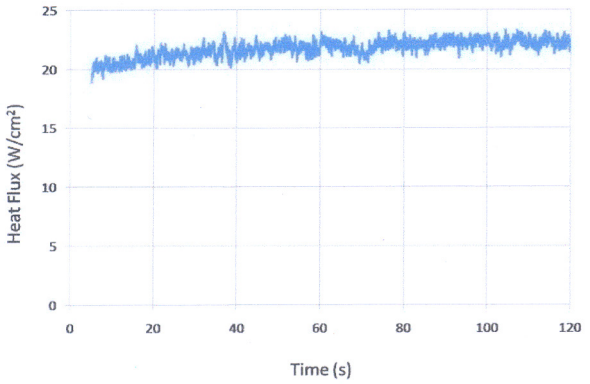

Fig.3 Heat Flux Measurements at 200 mm from Exit

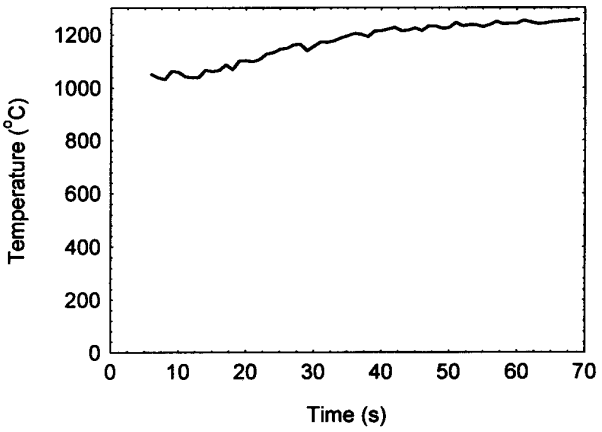

Fig.4 Plume Temperature Measurements at an Axial Location of 200 mm

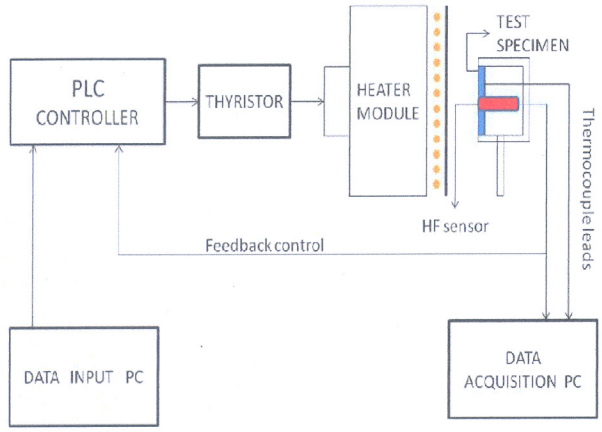

Fig.5 Block Diagram of Radiative Heating System

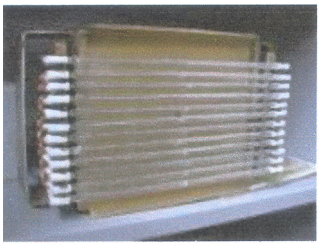

Fig.6 View of Radiative Heating System

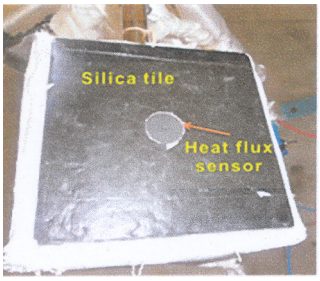

Fig.7 Photographic View of Silica Tile Flushed into Silica Tile Specimen

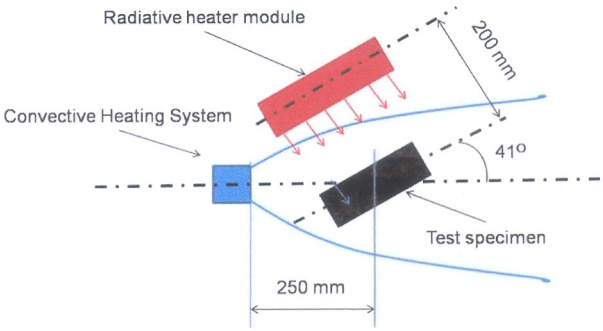

Fig.8 Schematic Diagram of Test Setup

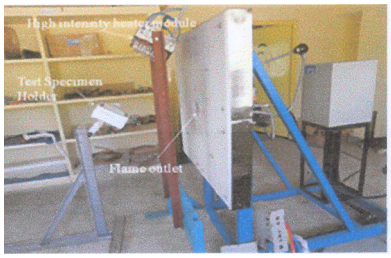

Fig.9 Pictorial View of Complete Test Setup

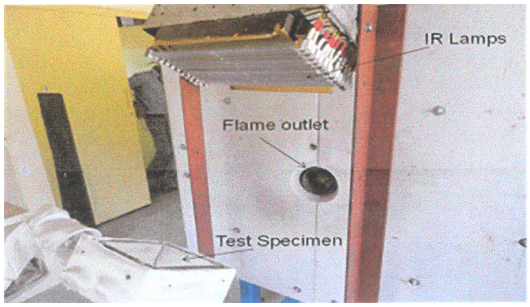

Fig.10 Pictorial View of IR Lamps Facing the Specimen Placed at the CHS Exit

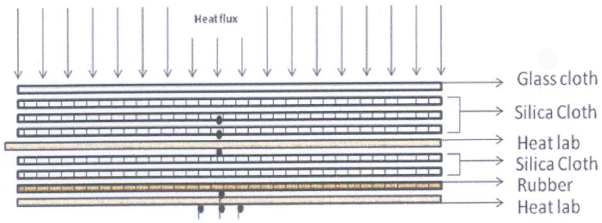

Fig.11 Configuration of Solid Motor Thermal Boot Test Specimen

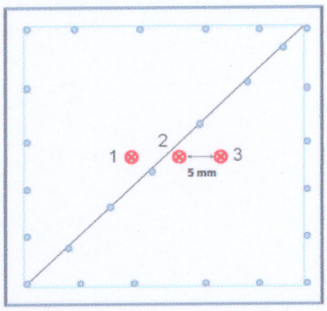

Fig.12 Thermocouple Locations Bonded on Backwall of the Specimen

Fig.13 Photographic View During Test

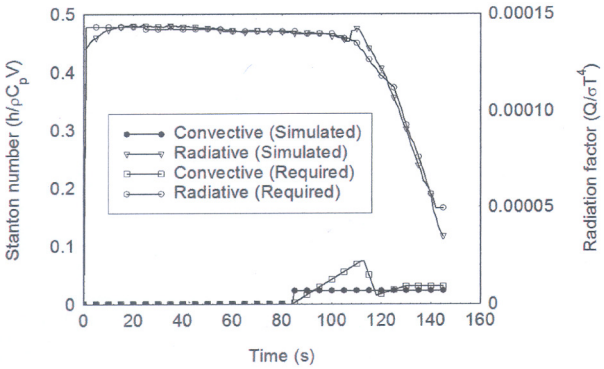

Fig.14 Comparison of Required and Simulated Heat Flux Histories

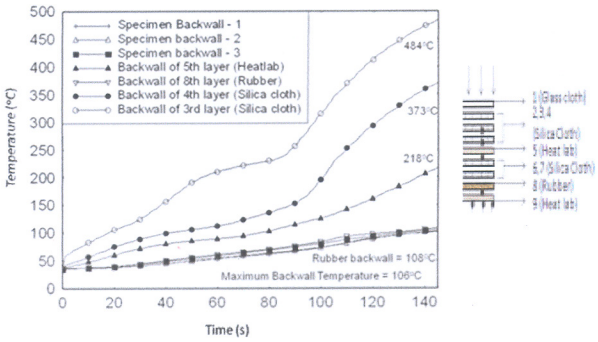

Fig.15 Thermal Response of Flexible Thermal Barrier

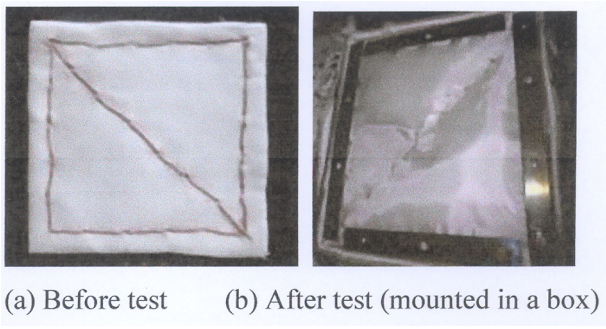

Fig.16 Photographic Views of Specimen